

Revaluation of the lower critical field in superconducting H₃S and LaH₁₀ (Nature Comm. 13, 3194, 2022).

V. S. Minkov¹, E. F. Talantsev^{2,3}, V. Ksenofontov¹, S. L. Bud'ko^{4,5}, F. F. Balakirev⁶, M. I. Erements¹

¹Max Planck Institute for Chemistry; Hahn Meitner Weg 1, Mainz 55128, Germany

²M.N. Mikheev Institute of Metal Physics, Ural Branch of the Russian Academy of Sciences, S. Kovalevskoy St 18, 620108 Ekaterinburg, Russian Federation

³NANOTECH Centre, Ural Federal University, Mira St 19, 620002 Ekaterinburg, Russian Federation

⁴Ames National Laboratory, U.S. Department of Energy, Iowa State University; Ames, IA 50011, United States

⁵Department of Physics and Astronomy, Iowa State University; Ames, IA 50011, United States

⁶Los Alamos National Laboratory; Los Alamos, NM 87545, USA

*Corresponding authors:

Email: m.eremets@mpic.de (M.I.E.); v.minkov@mpic.de (V.S.M)

In our paper¹, we studied the magnetic response of H₃S and LaH₁₀ superconductors to an applied magnetic field using Superconducting Quantum Interference Device (SQUID) magnetometry. Hirsch, in his comment², highlighted an inconsistency in the data averaging procedure while questioning whether high- T_c hydrides are superconductors at all. We accept the criticism regarding our method of extracting the penetration field H_p from the original data. Our SQUID magnet becomes noisy at high magnetic fields, which necessitated the smoothing of a small portion of the data. To eliminate any data processing issues, we have performed an alternative data analysis that does not require data smoothing to estimate the penetration field H_p values. The formulation of the analysis is identical to the one widely used for determining critical currents in superconductors³. Recently, it has been shown to work effectively for extracting H_p and the lower critical field H_{c1} from DC magnetization data⁴. The H_p values of the present analysis are consistent with those published in our original work¹. We wish to emphasise very clearly that the criticism pertains to the secondary issue of determining Ginzburg-Landau parameters for these hydride superconductors and does not undermine the validity of the existence of hydride superconductivity. Indeed, as part of our paper¹, we also published $m(H)$ curves demonstrating the virgin curve (about which the analysis issues were raised) followed by magnetic hysteretic loops that have the classic form of the hysteresis curves of superconductors. Above T_c , in both H₃S and LaH₁₀, the hysteresis is absent. We make all the data available so that readers can judge for themselves.

First, we take the opportunity to briefly review the status of work on hydride superconductivity, responding to inferences by Hirsch and co-workers that it is somehow not real.

The discovery of high-temperature superconductivity in hydrogen sulfide at $P \approx 150$ GPa, with a record critical temperature (T_c) of 203 K⁵, marked a milestone in superconductivity research and established a new family of materials known as hydrogen-rich superconductors^{6,7}. This family includes hydrides with different types of chemical bonding – covalent and metallic – between hydrogen and heavy atoms. All exhibit conventional superconductivity, allowing accurate T_c calculations for certain crystal lattices. Advances in crystal structure prediction have significantly accelerated the search for new, promising high- T_c superconductors⁷.

Despite the challenges of probing and studying superconductivity in samples with a size of tens micrometres within diamond anvil cells under extreme pressures, the existence of superconductivity in hydrogen-rich compounds is firmly established by various independent experimental techniques and independent research teams⁸. These compounds have achieved T_c values reaching 245 K in YH₉^{9,10} and 250 K in LaH₁₀¹¹⁻¹⁴.

Hydrogen-rich superconductors exhibit all necessary hallmarks of superconductivity, which have been probed under megabar pressures, and different research groups have well reproduced their properties⁸. High-temperature superconductivity at high pressures is evidenced by:

1. Zero electrical resistivity below T_c , or at least orders of magnitude lower than that of any known metal;

2. The Meissner state, involving the expulsion of an applied magnetic field from the sample upon cooling below T_c ;
3. The characteristic complex response of a superconductor to applied magnetic fields, which differs between type-I and type-II superconductors. For type-II superconductors, several phenomena are associated with the penetration of magnetic fields into the sample and include trapped magnetic flux, vortex creep, vortex lattice melting, a decrease in T_c with an increase in an applied magnetic field, and the suppression of superconductivity at magnetic fields above the upper critical field H_{c2} ;
4. Critical current density j_c , above which the resistance-less state disappears;
5. Superconducting energy gap indicating the collective nature of the charge carriers;
6. Pronounced isotope effect demonstrating the involvement of the crystal lattice in phonon-mediated superconductivity.

Studies of high-temperature superconductivity continue both theoretically, to better understand its high T_c and the prospects for room-temperature superconductivity, and experimentally, with many new superconductors being discovered⁶. The initially discovered superconductors H_3S and LaH_{10} have been characterized most thoroughly, with key superconducting parameters such as T_c , Ginzburg-Landau parameter, energy gap, coherence length ξ , London penetration depth λ_L , upper critical field H_{c2} , lower critical field H_{c1} , thermodynamic critical field H_c , and critical current density j_c estimated⁸.

Four-probe electrical transport measurements have been well developed for the use in diamond anvil cells and serve as a primary tool for detecting and studying superconductivity at high pressures. This method is routinely used in various laboratories^{8,12-18} and references herein. Another independent technique for proving and investigating superconductivity is magnetic susceptibility measurements⁵, which have recently been significantly improved for megabar high-pressure conditions⁸. Currently, three techniques are used for magnetic measurements at high pressures: a double modulation AC technique using a system of coils^{19,20}, SQUID magnetometry^{5,21}, and nitrogen-vacancy (NV) color centers implanted in diamond anvils as quantum sensors²². Additionally, the screening of applied magnetic fields by the H_3S superconductor has been explored using the forward nuclear resonant scattering technique, employing the ^{119}Sn Mössbauer isotope as a sensor²³.

The double modulation AC approach measures an anomaly in magnetic response and provides a value of T_c and a qualitative indication of the superconducting transition. This method is expected to be more widely used despite its relative complexity. This technique has detected the magnetic response arising from the superconducting nature of highly compressed hydrides such as H_3S ¹⁹ and LaH_{10} ²⁰. Another technique, static DC measurements using SQUID magnetometry, yields the absolute values of magnetic susceptibility. The development of miniature nonmagnetic diamond anvil cells^{1,5,21} and the trapped flux method²⁴ have significantly expanded the applicability of SQUID magnetometry.

The NV centers technique has also been successfully adapted to the megabar pressure range, demonstrating high sensitivity and submicron spatial resolution. These features enable the detection of magnetic response from much smaller samples, for instance, few-micrometers-size CeH_9 phase²². Ongoing development of the NV center technique aims to increase the range of applied magnetic fields used for measurements.

Next, we turn our attention to the magnetic flux penetration field which was one of the measured quantities in our paper¹. Currently, only DC measurements using SQUID magnetometry allow for the study of magnetic field penetration into a sample over a wide range of applied magnetic fields, enabling the estimation of H_p (magnetic flux penetration field) values. H_p is connected with the lower critical field, H_{c1} , via the demagnetization factor of the sample. The onset of applied magnetic field penetration into a superconductor is determined from the deviation of the virgin $m(H)$ magnetization curve from the linear response, which corresponds to the Meissner state.

To implement these measurements, a unique tiny DAC with a diameter of 8.8 mm was designed to perfectly fit the bore of commercial SQUIDs. The DAC body is made of materials with very low-magnetic susceptibility, yet it still significantly contributes to the recorded total signal. Nevertheless, the signal from the sample is clearly visible against the DAC background (see Figure 1a in ¹). This is remarkable because the mass of the DAC is approximately 10^8 times larger than that of the sample.

The screening of low applied magnetic fields, indicating the Meissner state, and the presence of hysteretic loops upon sweeping high applied magnetic fields, evidencing the presence of persistent superconducting currents, were clearly observed in H₃S samples in the pioneering work⁵. However, no initial $m(H)$ data, or so-called virgin curves, were measured, and H_{c1} and λ_L were only roughly estimated⁵.

Additionally, $m(H)$ magnetization data of H₃S at $P = 140$ GPa, including the virgin curve, were measured at a single temperature $T = 100$ K, using a magnetic property measurement system (MPMS) from Quantum Design, as reported in Ref.²¹ At that time, we performed conventional cleaning of the DAC body, diamond anvils, seats, and gaskets to remove possible contamination stemming from the manufacture of these parts using instruments made of steel and tungsten carbide (with impurities of cobalt). However, the conventional cleaning did not completely eliminate the strong paramagnetic contribution of the DAC assembly, which significantly affected the measured total signal. It should also be noted that this DAC had additional elements (electrical leads, wiring, and solder) for electrical transport measurements, which also contributed to the background. Therefore, to minimize the paramagnetic perturbation, we performed these measurements using a standard background subtraction procedure of the MPMS software for the SQUID magnetometer, where the background was collected above T_c at $T = 210$ K (see the inset in Figure 1). In our subsequent works^{1,24}, we succeeded in further development of post-machining cleaning procedures for the high-pressure DAC assembly (see below), and the background subtraction procedure was not applied for either $m(T)$ or $m(H)$ magnetic susceptibility measurements. More recently, the penetration of magnetic flux into H₃S and LaH₁₀ superconductors was systematically studied using the almost background-independent trapped flux method over a wide temperature range²⁴.

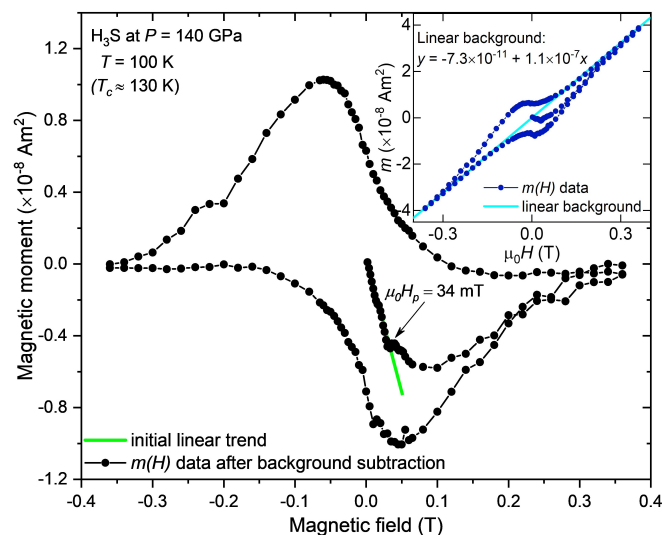


Figure 1. Magnetization $m(H)$ measurements in H₃S sample pressurized at $P = 140$ GPa ($T_c \approx 130$ K) from Ref.²¹, demonstrating typical superconducting behavior. Raw $m(H)$ data, including the background response from the DAC, are shown as blue circles in the inset. In this case, the background is paramagnetic, leading to a positive background slope in the raw data. After the subtraction of the background, approximated by a linear function (sky blue line in the inset), the $m(H)$ data exhibits the typical shape for a type-II superconductor. The virgin $m(H)$ curve shows a clear deviation from the initial linear trend (green line) at approximately 34 mT.

Our work¹ provided a significant step in understanding the behavior of H₃S and LaH₁₀ samples in applied magnetic fields, demonstrating not only the qualitative features of superconducting phase in these compounds, such as screening and expulsion of the applied magnetic field and the presence of hysteretic loops upon sweeping applied magnetic fields at temperatures below T_c , but also the estimation of several superconducting parameters such as the penetration field H_p and London penetration depth λ_L .

In our work¹ we made every effort to avoid all possible sources of contamination in our samples, which could lead to a paramagnetic background slope in magnetization $m(H)$ measurements. To achieve this, all elements of the high-pressure cell assembly were thoroughly etched in an ultrasonic cleaner with acids. All parts of the DACs and rhenium gaskets were etched in 3 M hydrochloric acid for 30 minutes, and the diamonds were etched in a mixture of concentrated nitric and hydrochloric acids in a 1:3 molar ratio for 90 minutes. As a result, the $m(H)$ data of DACs with the *Im-3m*-H₃S and *Fm-3m*-LaH₁₀ samples were not distorted by paramagnetic slope from impurities, and showed the diamagnetic slope naturally expected from the magnetic susceptibility values of the materials used for the high pressure assembly (see Figure 2).

At a number of temperatures, we measured $m(H)$ data by sweeping applied magnetic fields in the range of -1 to 1 Tesla to obtain hysteretic loops at temperatures above and below T_c of H₃S and LaH₁₀. Several such data are shown in Figure 2. Since each $m(H)$ loop measurement took several days, at some temperatures in our study we looked at only the virgin curve which is the part of relevance to obtaining H_p .

We estimated $\mu_0 H_{c1}$ values of ~ 0.82 T and ~ 0.55 T, and $\lambda_L(0)$ of ~ 20 nm and ~ 30 nm in H₃S and LaH₁₀, respectively, after considering the estimated geometry of the synthesized samples. The small values of λ_L indicate a high superfluid density in both hydrides. These compounds have the values of the Ginzburg-Landau parameter κ of ~ 12 – 20 and belong to the group of moderate- κ type-II superconductors (e.g., MgB₂ and A15 alloys), rather than being hard superconductors, as might be intuitively expected from their high T_c s. Our later estimated value of $\lambda_L(10\text{ K}) = 37$ nm in H₃S²⁴, does not alter this conclusion.

However, Hirsch, in his comment², expressed concerns about an inconsistency in the averaging of the data in our work¹. In the end of his comment, Hirsch escalated his concerns to absurd scepticism about the entire field of high- T_c conventional superconductivity.

A key point is how to determine the onset of the deviation of the virgin $m(H)$ part of the data from the linear trend in a case of noisy data that we had in minor instances. The source of the noise is the S700X SQUID magnetometer, which we used in all our experiments¹, it utilizes two current sources: the first provides magnetic fields up to 30 mT with low noise, and the second provides higher fields but with higher noise, especially in the field range of 35-150 mT. This design is standard from the manufacturer of the S700X SQUID magnetometer, and we cannot modify it. As a result, we had no problem with the signal-to-noise ratio and the estimation of H_p values when the onset point of deviation from the linear trend lies within the range of magnetic fields < 30 mT. Fortunately, this holds true for all measured data for the LaH₁₀ sample (and for the majority of well-known superconductors) and partly for the H₃S sample at $T = 180$ K and 160 K.

The deviation points for the H₃S sample measured at lower temperatures shift to the range of noisy data. The physical origin for this shift is a large value of the lower critical field, H_{c1} , in H₃S (or, in other words, short λ_L).

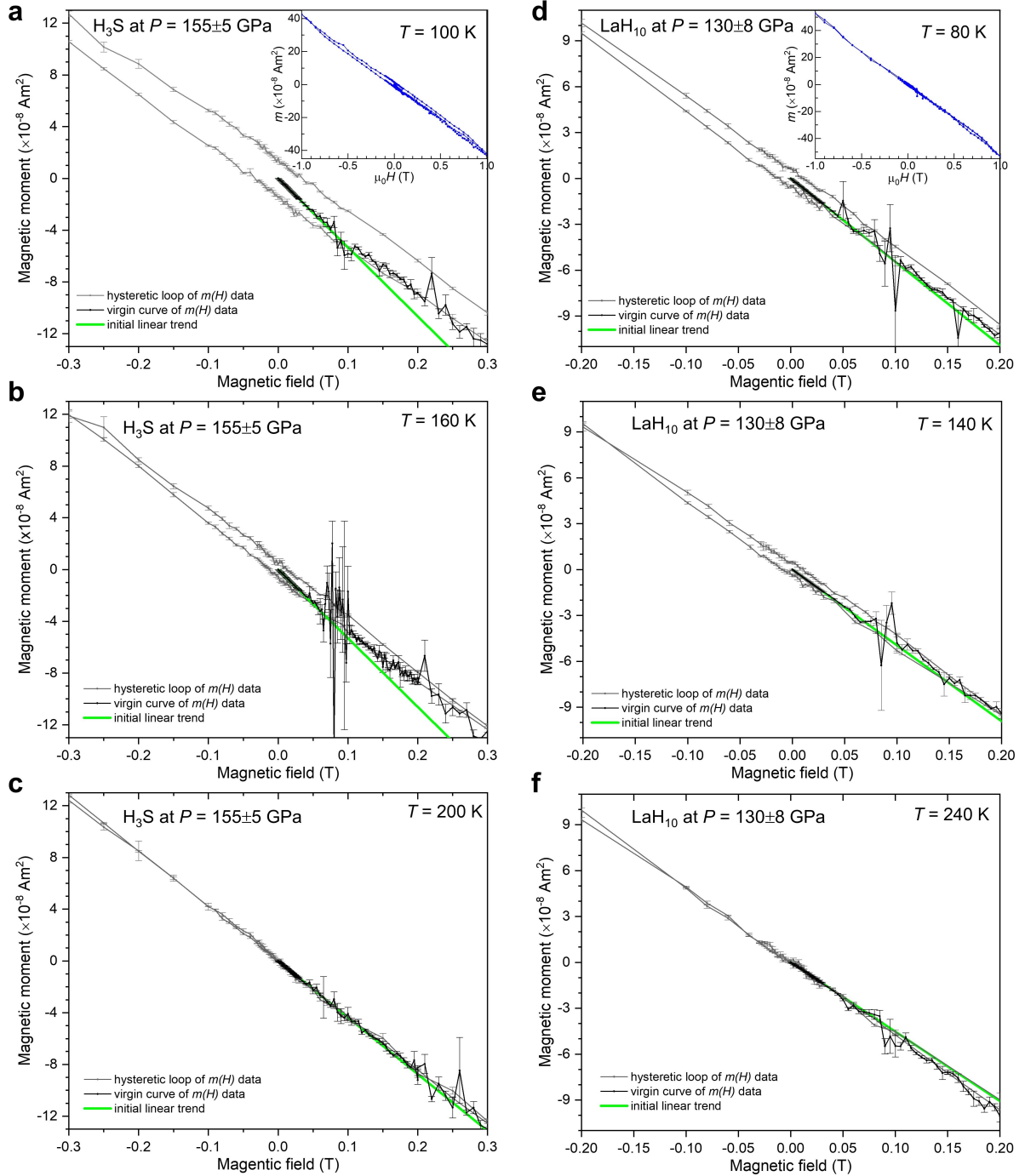


Figure 2. Magnetization $m(H)$ measurements in hydrogen-rich superconductors $Im\text{-}3m\text{-H}_3\text{S}$ and $Fm\text{-}3m\text{-LaH}_{10}$. $m(H)$ data upon sweeping applied magnetic fields in the range of -1 to 1 T, including virgin curves, demonstrate: (a, b) the presence of characteristic superconducting hysteresis at $T = 100$ K and 160 K (below T_c); and (c) the absence of the hysteresis at $T = 200$ K (above T_c) in the $Im\text{-}3m\text{-H}_3\text{S}$ sample pressurized at $P = 155\pm 5$ GPa. $m(H)$ data upon sweeping applied magnetic fields in the range of -1 to 1 T, including virgin curves, demonstrate: (d, e) the presence of characteristic superconducting hysteresis at $T = 80$ K and 140 K (below T_c); and (f) the absence of the hysteresis at $T = 240$ K (above T_c) in the $Fm\text{-}3m\text{-LaH}_{10}$ sample pressurized at $P = 130\pm 8$ GPa. Black and grey circles correspond to the virgin and hysteretic portion of the $m(H)$ data. Green lines represent the initial linear behaviour of the virgin $m(H)$ data and serve as a guide to demonstrate the deviation of the virgin curve from the linear trend. The measured $m(H)$ data showed a diamagnetic slope of the background of the rigorously etched DAC assembly. Insets demonstrate the whole measured range of $m(H)$ datasets for the H_3S sample at $T = 100$ K and the LaH_{10} sample at $T = 80$ K.

Even when the deviation is visible to the eye in the original scattered data, smoothing or averaging is required for an accurate and objective determination of H_p values. Therefore, we first smoothed the original data in the noisy range to combine it with the low-noise data for the systematic determination of the deviation from linear behavior. This is not a trivial problem, which we solved in several steps of smoothing/averaging. In retrospect, we accept that the procedure we used is indeed open to criticism. Therefore, we report an alternative method for processing the original measured data to estimate H_p without resorting to smoothing.

Since no standard approach to detecting H_p is found in the literature, the deviation from the initial linear trend is typically determined by eye. Another source of uncertainty in the determination of H_p in type-II superconductors, particularly those exhibiting strong pinning, arises from the absence of a dramatic change in the magnetic moment in virgin $m(H)$ magnetization curves when the applied magnetic field exceeds H_p . This task is even more challenging for hydrogen-rich compounds, as their useful superconducting response is close to the sensitivity limit of the SQUID magnetometer and is further perturbed by the background signal of the diamond anvil cell (DAC).

We recently developed a generalized method for systematically determining the deviation of a magnetization curve from linear behavior. An identical approach is widely used for the determination of the critical current values in superconductors³, and it has been successfully extended to extract H_p from *DC* magnetization data⁴ in various superconductors. This method is also attractive for us because datasets with variable noise levels can be easily analyzed.

The main idea of this method is to fit the measured $m(H_{appl})$ by the power-law function of the applied magnetic field H_{appl} . The power-law function includes a linear dependent term, which is attributed to the linear Meissner diamagnetic response. The deviation from the linear dependence is described by $m_c \times \left(\frac{H_{appl}}{H_p}\right)^n$ term, where m_c is the threshold criterion to define the H_p . Thus, m_c plays a similar role to the electric field criterion of $E_c = 1 \mu\text{V}/\text{cm}$ used to determine the transport critical current density³ from the E - J curves. The details of these methods can be found in Refs.^{3,4} A distinct advantage of this method is that it provides a systematic criterion for detecting H_p values based on phenomenologically established shape of the $m(H)$ dependence in the vicinity of H_p , whereas previously employed methods rely on a threshold value that varies widely from report to report and are therefore much less consistent. The fitting function is described by Equation (1):

$$m(H_{appl}) = m_0 + k \times H_{appl} + m_c \times \left(\frac{H_{appl}}{H_p}\right)^n \quad (1)$$

where m_0 is an instrumental offset, k is a linear term (also known as the Meissner slope), m_c is the threshold criterion, and n is the power-law exponent.

It should be noted that a power-law equation is not applicable for fitting the entire $m(H)$ magnetization curve and must be used solely to find the onset point where the measured magnetic moment starts to deviate from the initial linear trend due to the penetration of magnetic flux into the superconductor. For this reason, one should define m_c and the range of H_{appl} for reasonable fitting. Identical conditions exist in the determination of the critical current density from the E - J curves using the power-law approach.

For $m(H)$ datasets where H_p lies in the low-noise region, we set the m_c criterion as approximately three times the value of the uncertainty of the measured magnetic moment, above which the deviation from the linear trend becomes reliable. We limited the range of $m(H)$ data for the fitting to the value of H_{appl} at which the difference between the measured $m(H_{appl})$ and the Meissner line (linear term) reached approximately ten times the value of m_c .

We show several such fits with fitting parameters in Figure 3 and Supplementary Figure 1. For better representation of the onset of H_p , we subtracted the linear background $y = a + bx$ (a and b parameters given for each plot). We also reanalyzed the value of H_p for the H₃S data at $P \approx 140$ GPa ($T_c \approx 140$ K) published in Ref.²¹ The H_p values refined by the new approach are consistent with those estimated in the original works^{1,21}.

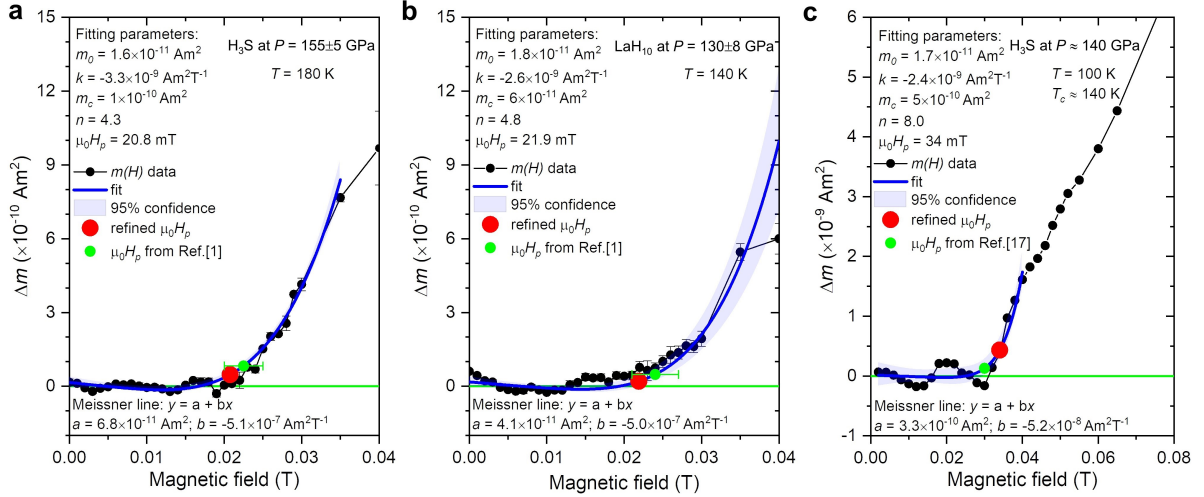


Figure 3. The extraction of H_p in the low-noise region of applied magnetic fields (≤ 30 mT). (a) A portion of the $m(H)$ virgin curve for the $Im-3m$ -H₃S sample at $P = 155 \pm 5$ GPa, measured at $T = 180$ K from Ref.¹; (b) a portion of the $m(H)$ virgin curve for the $Fm-3m$ -LaH₁₀ sample at $P = 130 \pm 8$ GPa, measured at $T = 140$ K from Ref.¹; (c) a portion of the $m(H)$ virgin curve for the H₃S sample at $P \approx 140$ GPa ($T_c \approx 140$ K), measured at $T = 100$ K from Ref.²¹ We subtracted the linear function of $y = a + bx$ (with a and b parameters shown below each curve) from the original $m(H)$ data for better presentation of the initial linear trend. This line represents the Meissner line and is defined as linear fit of the data measured at low applied magnetic fields below H_p . Black circles represent the measured $m(H)$ data; red and green circles represent H_p values estimated in the present work and in Refs.^{1,21}, respectively. The green line depicts the Meissner line ($y = 0$), and blue curves represent the fits with 95% confidence bands.

For $m(H)$ datasets of the $Im-3m$ -H₃S sample at $P = 155 \pm 5$ GPa measured at $T \leq 140$ K, where H_p values lie above 30 mT (in the noisy region), we set the m_c criterion to approximately the averaged value of uncertainties of the $m(H_{appl})$ datasets used for fitting, including both low- and high-noise regions, but not larger than 10% of the maximum diamagnetic response $|\Delta m_{max}|$ from the superconducting H₃S sample. Thus, for the dataset measured at $T = 140$ K, $m_c = 8 \times 10^{-10} \text{ Am}^2$ and for the datasets measured at $T \leq 120$ K, $m_c = 1 \times 10^{-9} \text{ Am}^2$. The data range for fitting was limited to magnetic fields at which the difference between the measured $m(H_{appl})$ and the Meissner line (linear term) reached approximately ten times the value of m_c , as it was done for the estimation of H_p in the low-noise region. We show these fits with fitting parameters in Figure 4 and Supplementary Figure 2.

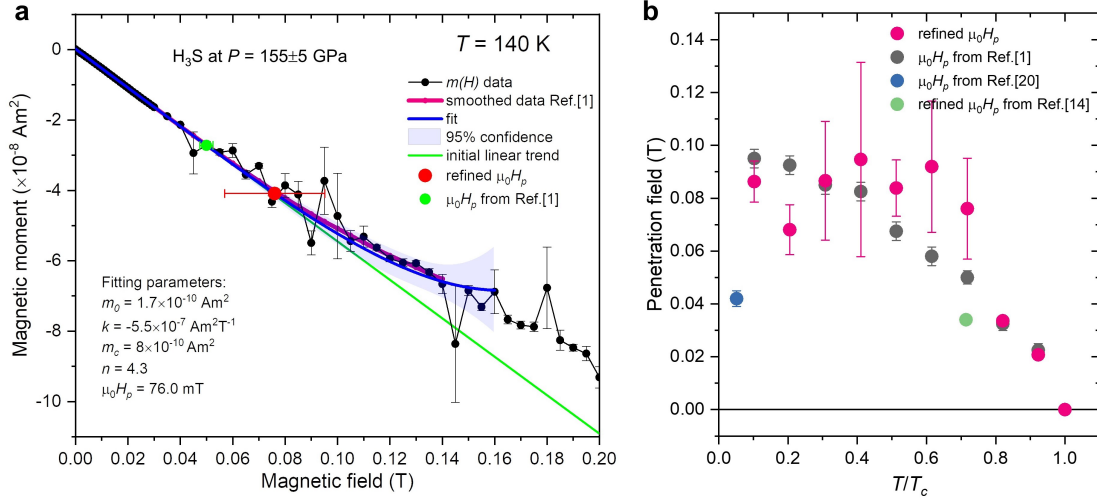


Figure 4. The extraction of H_p in the high-noise region of applied magnetic fields (> 30 mT) for the *Im-3m*-H₃S sample at $P = 155\pm 5$ GPa. (a) Fit of the portion of the $m(H)$ virgin curve for the *Im-3m*-H₃S sample at $P = 155\pm 5$ GPa, measured at $T = 140$ K by Equation (1). Fitting parameters are shown on the panel. The smoothed data from Ref.¹ are shown as magenta curve. The initial linear trend was defined as a linear fit of the measured data in the applied magnetic fields region of 0-20 mT. (b) Summary plot of the estimated H_p values for H₃S samples measured in different experiments: traditional magnetic susceptibility measurements (grey circles from Ref.¹ and green circle from Ref.²¹) and trapped magnetic flux method (blue circle, Ref.²⁴).

In traditional magnetization measurements, the total magnetic signal from the pressurized sample unavoidably includes the response of the DAC body. The diamagnetic response of the DAC continuously grows with applied magnetic fields, while the useful signal from the superconducting sample weakens soon after H_{appl} exceeds H_p . This leads to a decrease in the signal-to-background ratio at high applied magnetic fields, but does not affect the estimation of H_p values.

Another important parameter is the background response of DACs to applied magnetic fields. Despite our efforts to manufacture miniature DACs with a background response to applied magnetic fields as low as possible, in practice, the background of the entire high-pressure assembly is not perfectly linear at low applied magnetic fields and across a wide temperature range. Since we cannot significantly increase the size of superconducting samples (the larger diamond anvil culets do not sustain these pressures) to improve the useful signal-to-background ratio, the subtle nonlinearity of the DAC background can manifest in the $m(H)$ measurements. However, this feature does not significantly affect the detection of superconductivity in our samples. Several cases for the background dependence of the DAC used in our work¹ at $T = 20$ K, 180 K, and 200 K are shown in Supplementary Figure 3. When the sample is in the normal state at 200 K, the virgin $m(H)$ curve shows a subtle downturn at approximately 10 mT. The same effect is observed for the data measured at lower temperatures, where $\mu_0 H_p$ values exceed 30 mT, i.e., when the nonlinear DAC background interferes with the Meissner state of the superconducting sample (linear magnetic field dependence of the $m(H_{appl})$). At temperatures where $\mu_0 H_p$ is below 30 mT, the effect of the penetration of the magnetic flux into the superconducting sample surpasses the nonlinearity in the DAC background, allowing for estimation of H_p .

We also checked the variation of H_p values upon changing the range of the $m(H)$ dataset used for fitting. By extending the H_{appl} range to two times ($\mu_0 H_{appl} = 300$ mT) and three times ($\mu_0 H_{appl} = 440$ mT) for H₃S sample at $T = 100$ K, the exponent of the fitting function reduces from $n = 5$ to $n = 2.2$, resulting in less accurate fitting of the experimental data. Despite this, the extracted $\mu_0 H_p$ values do not change significantly: from 84 ± 10 mT to 63 ± 9 mT, a difference of approximately 25%. The value of $\mu_0 H_p$ reported in Ref.¹ is 68 ± 4 mT.

Applying the method proposed for the extraction of H_p from DC magnetization measurements in Ref.⁴ to our datasets for the $Im-3m$ -H₃S and $Fm-3m$ -LaH₁₀ samples reported in Ref.¹, we obtained the refined values summarized in Figure 5. In particular, the refined $\mu_0 H_p(0 K) = 108 \pm 7$ mT for the $Im-3m$ -H₃S sample at $P = 155 \pm 5$ GPa and 35 ± 3 mT for the $Fm-3m$ -LaH₁₀ sample at $P = 130 \pm 8$ GPa versus 97 ± 2 mT and 39 ± 2 mT for the datasets reported in Ref.¹

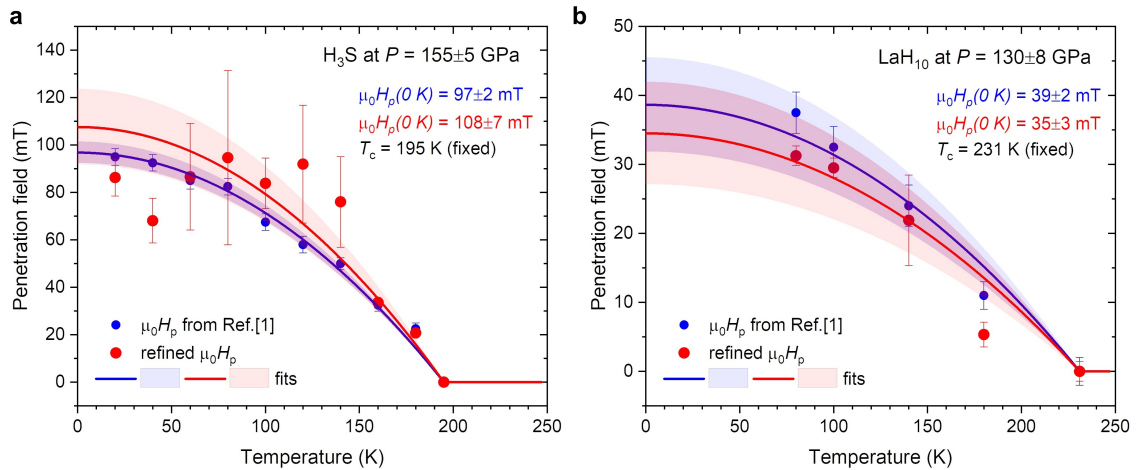


Figure 5. Temperature dependence of estimated H_p for the $Im-3m$ -H₃S and $Fm-3m$ -LaH₁₀ samples. (a) Refined H_p values for the $Im-3m$ -H₃S sample at $P = 155 \pm 5$ GPa; and (b) refined H_p values for the $Fm-3m$ -LaH₁₀ sample at $P = 130 \pm 8$ GPa. H_p values reported in Ref.¹ are shown grey circles. Fit of both datasets of estimated $H_p(T)$ values and their extrapolation to $H_p(0 K)$ was done using equation $H_p(T) = H_p(0 K) \times \left(1 - \left(\frac{T}{T_c}\right)^2\right)$. Blue and red circles represent the data from Ref.¹ and the refined data in the present work, respectively. Light blue and light red areas show 95% confidence bands of the fits.

It is noteworthy that estimating $H_{c1}(T)$ values necessitates knowing the demagnetizing factor, N . We derived the demagnetization correction, $(1-N)^{-1}$, from the estimated geometry of the synthesized samples, approximately 8.5 and 13.5 for H₃S and LaH₁₀, respectively. These values assume that the superconducting phases are uniform and shaped as ideal thin solid disks. However, the real sample shape and continuity of the superconducting phase can differ from this ideal case, with the worst scenarios being the sample consisting of separated small crystallites, which could reduce the demagnetization correction to the value of 1.5, or the superconducting regions being thinner than the idealised disks, in which case it could be substantially larger than our estimates. The systematic errors on our estimates of $H_{c1}(T)$ are therefore substantial, but we believe that the estimate is worth attempting, because $\kappa \sim \sqrt{H_{c2}/H_{c1}}$ so a valuable estimate of κ can be made even in the presence of large uncertainty in H_{c1} , and it is important to know approximately how strongly type-II the hydride superconductors are. The uncertainty in the real value of the demagnetizing factor is not specific to high-pressure measurements but also exists in ambient pressure studies, particularly for polycrystalline samples (e.g., see Figure 5 in Ref.²⁵).

In summary, it is crucial to re-emphasize that we have significantly advanced experimental techniques for studying the properties of novel hydrogen-rich high-temperature superconductors at high pressures using SQUID magnetometry^{1,5,21,23,24}. In particular, by utilizing traditional magnetic susceptibility^{1,5,21,23} and new trapped flux²⁴ methods, we have demonstrated the presence of all 7 hallmarks of superconductivity in these compounds:

- 1) Screening and expulsion of the applied magnetic field by the superconducting phase below its T_c ;
- 2) The appearance of hysteretic loops by sweeping the applied magnetic field at temperatures below T_c , related to persistent superconducting currents in superconductors and their growth with decreasing T ;

- 3) The existence of an initial linear trend of $m(H)$ in the virgin curve of magnetization data, related to the Meissner state of superconductors;
- 4) Trapping of magnetic flux by superconductors after switching off the applied magnetic field;
- 5) Different behaviours in the trapping of magnetic flux under zero-field-cooled and field-cooled protocols arising from the influence of the Meissner state of superconductors;
- 6) The presence of horizontal temperature-independent plateaus in $m_{trap}(T)$ measurements upon reverse cooling superconductors at temperatures below their T_c s;
- 7) Extremely slow creep of the trapped magnetic flux.

In addition, it should be mentioned that the reproducibility and consistency of our results between different magnetic measurements are notable. Both H_3S and LaH_{10} samples were also measured by trapped flux method²⁴, and the results obtained by two different techniques agree well with each other. Furthermore, the trapped flux method also provides the estimate of $\mu_0 H_p(10\text{ K}) = 42 \pm 3$ mT in H_3S at $P = 155 \pm 5$ GPa (diamond anvils in the DAC with LaH_{10} sample were destroyed during measurements), which we consider more accurate since the background of the DAC did not perturb the response of the superconducting sample. The estimations of H_p done by these two methods are consistent. It should be mentioned that in the literature, even ambient pressure superconductors demonstrate much larger dispersion in H_p .

In the present manuscript, we refined $H_p(T)$ values for the $Im-3m-H_3S$ and $Fm-3m-LaH_{10}$ samples by using an alternative method for determining the deviation from linear behaviour in applied magnetic fields in a more consistent manner. The refined $H_p(T)$ values are commensurate with the previously reported values in Ref.¹, and fitting curves of the $H_p(T)$ datasets to the Ginzburg-Landau critical field equation lie within the 95% confidence bands.

In addressing the broader suspicion raised about the validity of the whole hydride field of research by Hirsch and co-workers, we refer not just to our own work but to the multiple independent confirmations of hydride superconductivity by other groups, with the significant papers included in the citation list of this article.

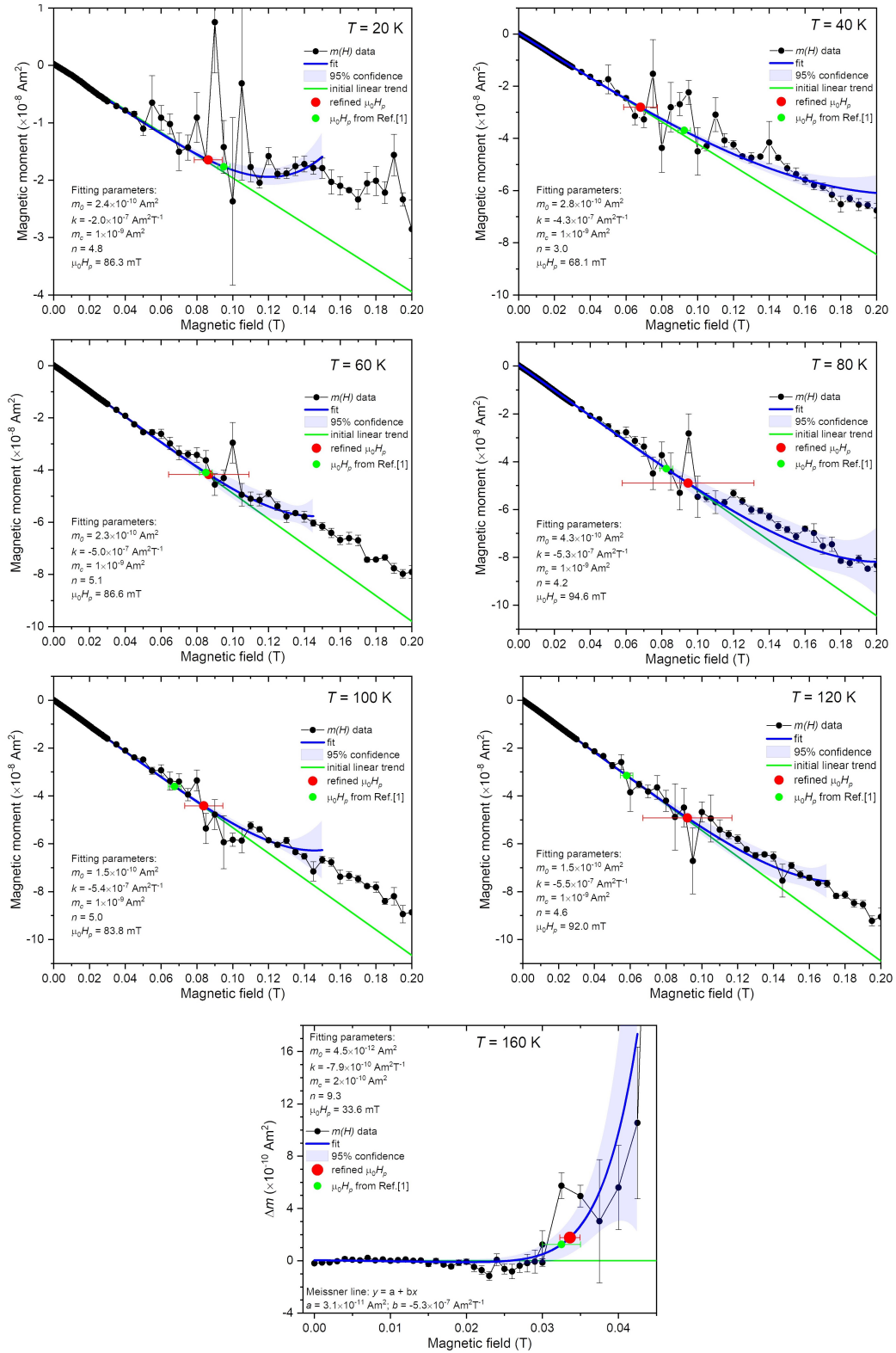
Acknowledgements

Authors are grateful to A. Mackenzie for helpful discussions. M.I.E. is thankful to the Max Planck community for valuable support and U. Pöschl for the encouragement. The National High Magnetic Field Laboratory is supported by the National Science Foundation through NSF/DMR-2128556, the State of Florida, and the U.S. Department of Energy. S.L.B. was supported by the U.S. Department of Energy, Office of Basic Energy Science, Division of Materials Sciences and Engineering under Contract No. DE-AC02-07CH11358. E.F.T. thanks financial support provided by the Ministry of Science and Higher Education of Russia within the theme “Pressure” No. 122021000032-5 and under Ural Federal University Program of Development within the Priority-2030 Program.

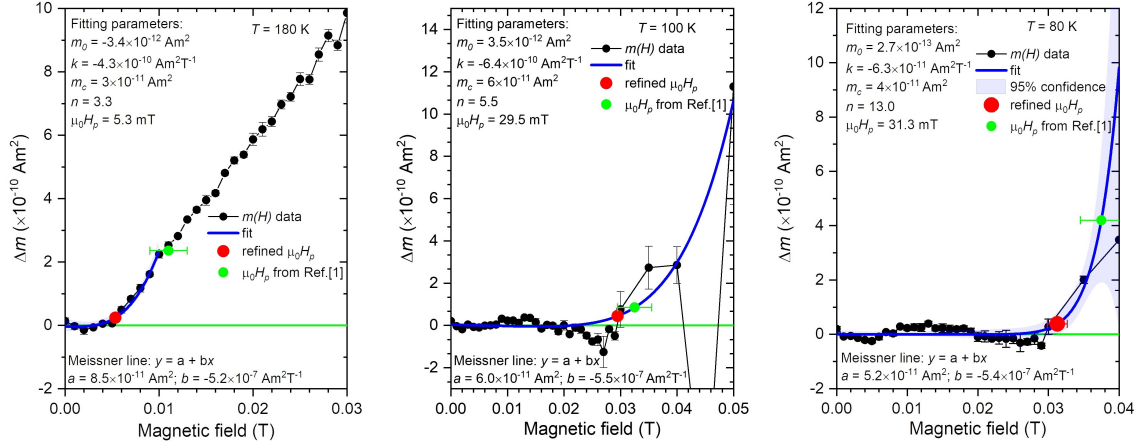
Data Availability

The data supporting the findings of this study are openly available at the Open Science Framework (<https://osf.io/7wqxb/>) with DOI 10.17605/OSF.IO/7WQXB.

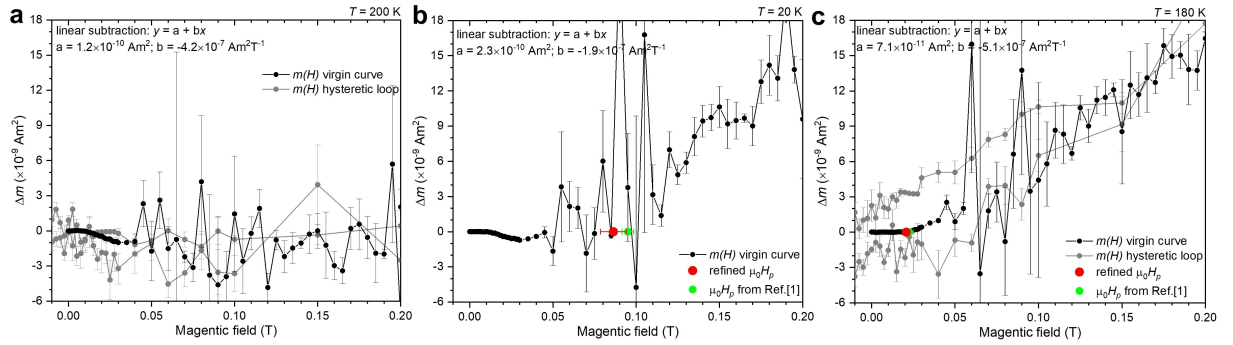
Supplementary Materials



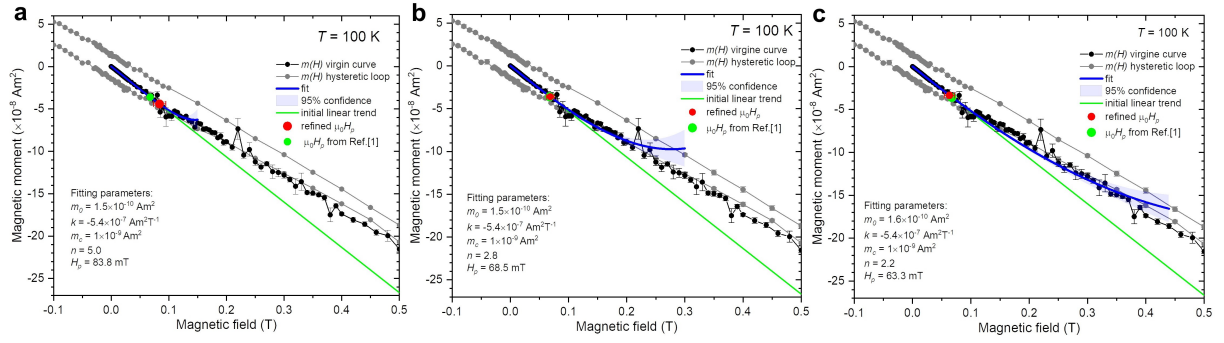
Supplementary Figure 1. The extraction of H_p from $m(H)$ magnetization data of the $Im\bar{3}m$ - H_3S sample at $P = 155 \pm 5 \text{ GPa}$. Black circles represent the measured $m(H)$ data; red and green circles represent H_p values estimated in the present work and in Ref.¹, respectively. The green line depicts the initial Meissner linear trend of the virgin curve in the Meissner state. This Meissner line is defined as linear fit of the data measured at low applied magnetic fields ($\leq 30 \text{ mT}$) and serves as a guide for the eye. Blue curves represent fits with 95% confidence bands.



Supplementary Figure 2. The extraction of H_p from $m(H)$ magnetization data of the $Fm-3m-LaH_{10}$ sample at $P = 130 \pm 8$ GPa in the low-noise region of applied magnetic fields (≤ 30 mT). We subtracted the linear function $y = a + bx$ (with a and b parameters shown below each curve) from the original $m(H)$ data for better presentation of the initial linear trend of the virgin curve. Black circles represent the measured $m(H)$ data; red and green circles represent H_p values estimated in the present work and in Ref.¹, respectively. The green line depicts the Meissner line ($y = 0$), and blue curves represent the fits with 95% confidence bands.



Supplementary Figure 3. Nonlinearity of the background of the diamond anvil cell with the $Im-3m-H_3S$ sample at $P = 155 \pm 5$ GPa in the region of applied magnetic fields below 30 mT. (a) $m(H)$ data measured at $T = 200$ K (above T_c of the superconducting H_3S sample) characterize the DAC background, showing a subtle downturn at approximately 10 mT. Importantly, this effect has the opposite sign compared to the penetration of magnetic flux into the superconducting sample at temperatures below T_c . (b) $m(H)$ data measured at $T = 20$ K demonstrate the same downturn from the DAC background, preceding the entrance of magnetic flux into the sample. This indicates that the $\mu_0 H_p$ value lies beyond 30 mT. (c) $m(H)$ data measured at $T = 180$ K indicate that the onset of magnetic flux penetration into the sample occurs at low applied magnetic fields (below 30 mT). In this case, the DAC background does not significantly affect the determination of the H_p value. To better demonstrate the nonlinear behaviour of the DAC at low magnetic fields, we subtracted the linear background from the measured $m(H)$ data. The coefficients of the function $y = a + bx$ are obtained by linear fit to the very initial portion of the virgin $m(H)$ dataset ($0 < \mu_0 H_{app} < 10$ mT) and are provided in each panel. Black circles represent the virgin portion of the $m(H)$ data; grey circles correspond to the hysteretic portion of the $m(H)$ data; green and red circles correspond to the refined values of H_p (where applicable).



Supplementary Figure 4. Influence of the range of the $m(H)$ dataset of the $Im-3m-H_3S$ sample ($P = 155 \pm 5$ GPa) measured at $T = 100$ K on H_p values upon fitting (when $\mu_0 H_p$ lies in the region of applied magnetic fields above 30 mT). (a) The fitting of the virgin curve of the $m(H)$ data is limited by $\mu_0 H_{appl} = 150$ mT, at which the difference between the measured $m(H_{appl})$ and the Meissner line reaches approximately ten times the value of m_c . The refined $\mu_0 H_p = 84 \pm 10$ mT. (b) The fitting of the virgin $m(H)$ data is extended to double the range, limited by $\mu_0 H_{appl} = 300$ mT. In this case, the refined $\mu_0 H_p = 68 \pm 6$ mT. (c) The results of the fitting when the selected $m(H)$ dataset is limited by $\mu_0 H_{appl} = 440$ mT. The refined $\mu_0 H_p = 63 \pm 9$ mT. Black circles represent the measured $m(H)$ data of the virgin magnetization curve; grey circles represent the hysteretic portion of the $m(H)$ data; red and green circles represent H_p values estimated in the present work and in Ref.¹, respectively. The green line refers to the initial linear trend (Meissner line), and blue curves represent the fits with 95% confidence bands.

References

1. Minkov, V. S. et al. Magnetic field screening in hydrogen-rich high-temperature superconductors. *Nat. Commun.* **13**, 3194 (2022).
2. Hirsch, J. E. Hysteresis loops in measurements of the magnetic moment of hydrides under high pressure: Implications for superconductivity. *Physica C: Superconductivity and its Applications* **617**, 1354449 (2024).
3. Wimbush, S. C. & Strickland, N. M. A Public Database of High-Temperature Superconductor Critical Current Data. *IEEE Transactions on Applied Superconductivity* **27**, 1-5 (2017).
4. Talantsev, E. F. Method to extracting the penetration field in superconductors from DC magnetization data. *Review of Scientific Instruments* **93**, 053912 (2022).
5. Drozdov, A. P., Erements, M. I., Troyan, I. A., Ksenofontov, V. & Shylin, S. I. Conventional superconductivity at 203 K at high pressures. *Nature* **525**, 73 (2015).
6. Sun, Y., Zhong, X., Liu, H. & Ma, Y. Clathrate metal superhydrides under high-pressure conditions: enroute to room-temperature superconductivity. *National Science Review* (2023).
7. Flores-Livas, J. A. et al. A perspective on conventional high-temperature superconductors at high pressure: Methods and materials. *Phys. Rep.* **856**, 1-78 (2020).
8. Erements, M. I., Minkov, V. S., Drozdov, A. P. & Kong, P. P. The characterization of superconductivity under high pressure. *Nature Materials* **23**, 26-27 (2024).
9. Kong, P. P. et al. Superconductivity up to 243 K in yttrium hydrides under high pressure. *Nature Communications* **12**, 5075 (2021).
10. Wang, Y. et al. Synthesis and superconductivity in yttrium superhydrides under high pressure. *Chinese Physics B* **31**, 106201 (2022).
11. Drozdov, A. P. et al. Superconductivity at 250 K in lanthanum hydride under high pressures *Nature* **569**, 528 (2019).
12. Somayazulu, M. et al. Evidence for superconductivity above 260 K in Lanthanum superhydride at megabar pressures. *Phys. Rev. Lett.* **122**, 027001 (2019).
13. Semenok, D. V. et al. Superconductivity at 253 K in Lanthanum–Yttrium ternary hydrides. *Mater. Today* **48**, 18-28 (2021).
14. Hong, F. et al. Superconductivity of Lanthanum superhydride investigated using the standard four-probe configuration under high pressures. *Chin. Phys. Lett.* **37**, 107401 (2020).
15. Nakao, H. et al. Superconductivity of Pure H₃S Synthesized from Elemental Sulfur and Hydrogen. *J. Phys. Soc. Jpn.* **88**, 123701 (2019).
16. Osmond, I. et al. Clean-limit superconductivity in synthesized from sulfur and hydrogen donor ammonia borane. *Physical Review B* **105**, L220502 (2022).
17. Cross, S. et al. High-temperature superconductivity in La₄H₂₃ below 100 GPa. *Phys. Rev. B* **109**, L020503 (2024).
18. Sun, Y., Zhong, X., Liu, H. & Ma, Y. Clathrate metal superhydrides under high-pressure conditions: enroute to room-temperature superconductivity. *National Science Review* **11**: nwad270 (2024).
19. Huang, X. et al. High-temperature superconductivity in sulfur hydride evidenced by alternating-current magnetic susceptibility. *National Science Review* **6**, 713-718 (2019).
20. Struzhkin, V. et al. Superconductivity in La and Y hydrides: remaining questions to experiment and theory. *Matter Radiat. Extremes* **5**, 028201 (2020).
21. Erements, M. I. et al. High-temperature superconductivity in hydrides: experimental evidence and details. *J. Supercond. Nov. Magn.* **35**, 965-977 (2022).
22. Bhattacharyya, P. et al. Imaging the Meissner effect in hydride superconductors using quantum sensors. *Nature* **627**, 73-79 (2024).
23. Troyan, I. et al. Observation of superconductivity in hydrogen sulfide from nuclear resonant scattering. *Science* **351**, 1303 (2016).

24. Minkov, V. S., Ksenofontov, V., Bud'ko, S. L., Talantsev, E. F. & Erements, M. I. Magnetic flux trapping in hydrogen-rich high-temperature superconductors. *Nature Physics* **19**, 1293-1300 (2023).
25. Matthews, G. A. B. et al. Effect of the sintering temperature on the microstructure and superconducting properties of MgB₂ bulks manufactured by the field assisted sintering technique. *Superconductor Science and Technology* **33**, 054003 (2020).